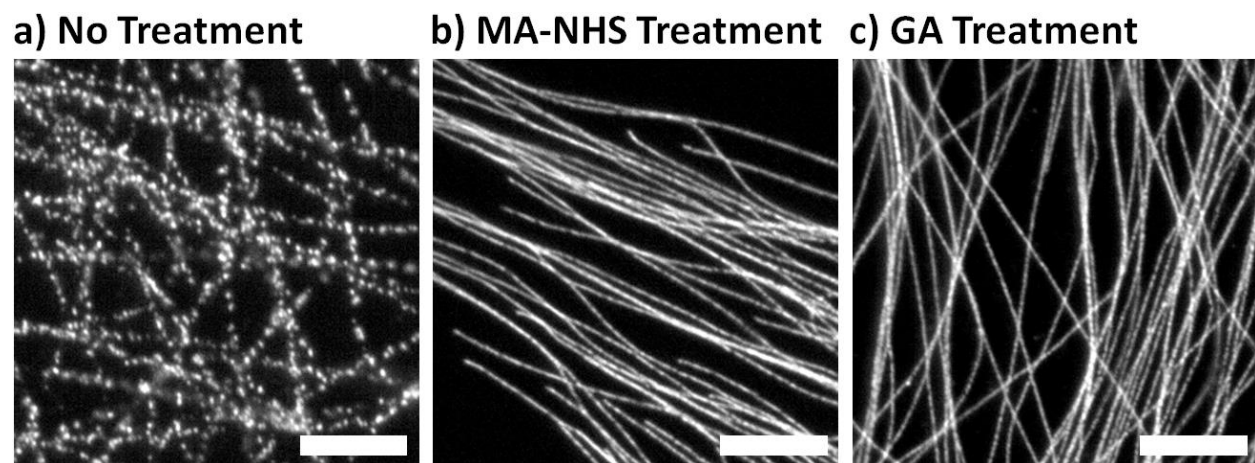


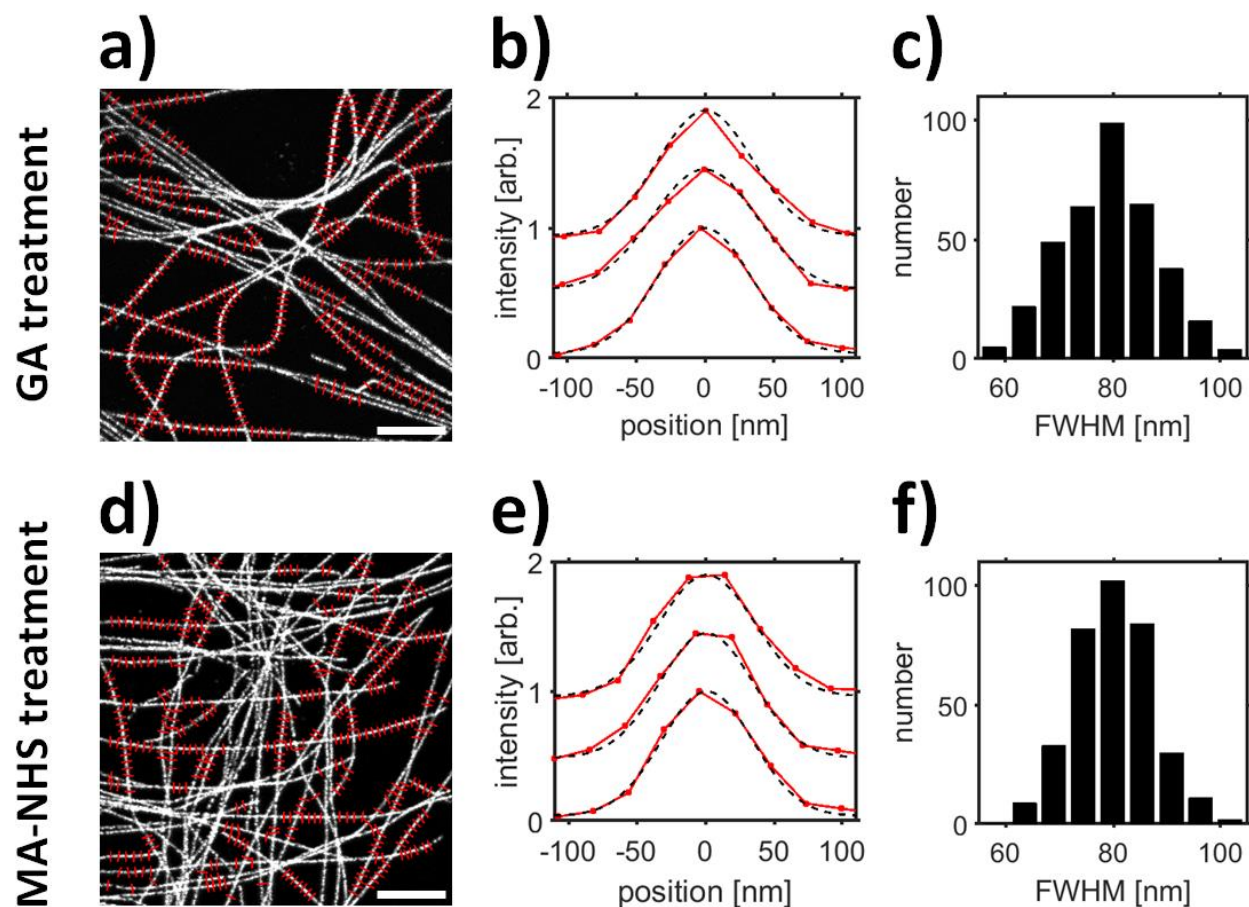
## Supplementary Information for “Expansion Microscopy with Conventional Antibodies and Fluorescent Proteins”

Figure	Result
<b>Supplementary Figure 1</b>	Post-stain treatment with MA-NHS or GA retains fluorescence for cells immunostained with conventional secondary antibodies.
<b>Supplementary Figure 2</b>	Measurement of ~80 nm microtubule profile for MA-NHS and GA treated cells immunostained for tubulin and estimate of ~65 nm resolution.
<b>Supplementary Figure 3</b>	Quantification of expansion fidelity for conventionally immunostained cell treated post-stain with MA-NHS and imaged by confocal microscopy.
<b>Supplementary Figure 4</b>	Quantification of expansion fidelity for cell immunostained with DNA-labeled secondary antibodies and imaged by confocal microscopy.
<b>Supplementary Figure 5</b>	Quantification of expansion fidelity for conventionally immunostained cell treated post-stain with GA; imaged pre-expansion by super-resolution microscopy and post-expansion by epifluorescence microscopy.
<b>Supplementary Figure 6</b>	Comparison of correlated pre- and post-expansion images of spindle-chromosome attachments.
<b>Supplementary Figure 7</b>	Explanation of image processing procedures used in <b>Fig. 2 e-f</b> .
<b>Supplementary Figure 8</b>	Quantification of expansion fidelity in three dimensions for conventionally immunostained cell treated post-stain with GA.
<b>Supplementary Figure 9</b>	Gallery of expanded cells immunostained for various structures and treated with GA prior to gelation, digestion, and expansion.
<b>Supplementary Figure 10</b>	Use of MA-NHS or GA treatment with conventional secondary antibodies leads to equal or brighter signal compared to DNA-antibody.
<b>Supplementary Figure 11</b>	Fluorescence retention measurements of GA, GFP-GA, MA, and DNA methods presented in this work.
<b>Supplementary Figure 12</b>	Comparison of fluorescence images of expanded cells immunostained with home-made or commercially available conventional fluorescently-labeled secondary antibodies.
<b>Supplementary Figure 13</b>	GA treatment of cultured cells permits short digestion times without expansion artifacts.
<b>Supplementary Figure 14</b>	MA-NHS treatment of cultured cells requires long-digestion times to avoid expansion artifacts.

<b>Supplementary Figure 15</b>	Short digestion times favor retention of intrinsic GFP signal in cultured cells.
<b>Supplementary Figure 16</b>	Treatment with GA favors retention of intrinsic GFP signal in cultured cells.
<b>Supplementary Figure 17</b>	Post-stain treatment with MA-NHS or GA retains fluorescence for mouse brain tissue immunostained with conventional secondary antibodies.
<b>Supplementary Figure 18</b>	Gallery of zoom-in views of synapses from <b>Fig. 3</b> .
<b>Supplementary Figure 19</b>	Quantification of expansion fidelity for brain tissue treated post-stain with MA-NHS and imaged by confocal microscopy.
<b>Supplementary Figure 20</b>	MA-NHS treatment retains fluorescent protein signal in mouse brain slices while no treatment has poor fluorescence retention.
<b>Supplementary Figure 21</b>	Gallery of expanded cells immunostained for nuclear DNA or tubulin using a range of fluorophores attached to antibodies.
<b>Supplementary Video 1</b>	3D rendering of expanded brain tissue from <b>Fig. 3</b> .
<b>Supplementary Table 1</b>	Detailed summary of sample preparation and imaging conditions.
<b>Supplementary Protocol 1</b>	Detailed protocol for magnification calculation and distortion analysis.

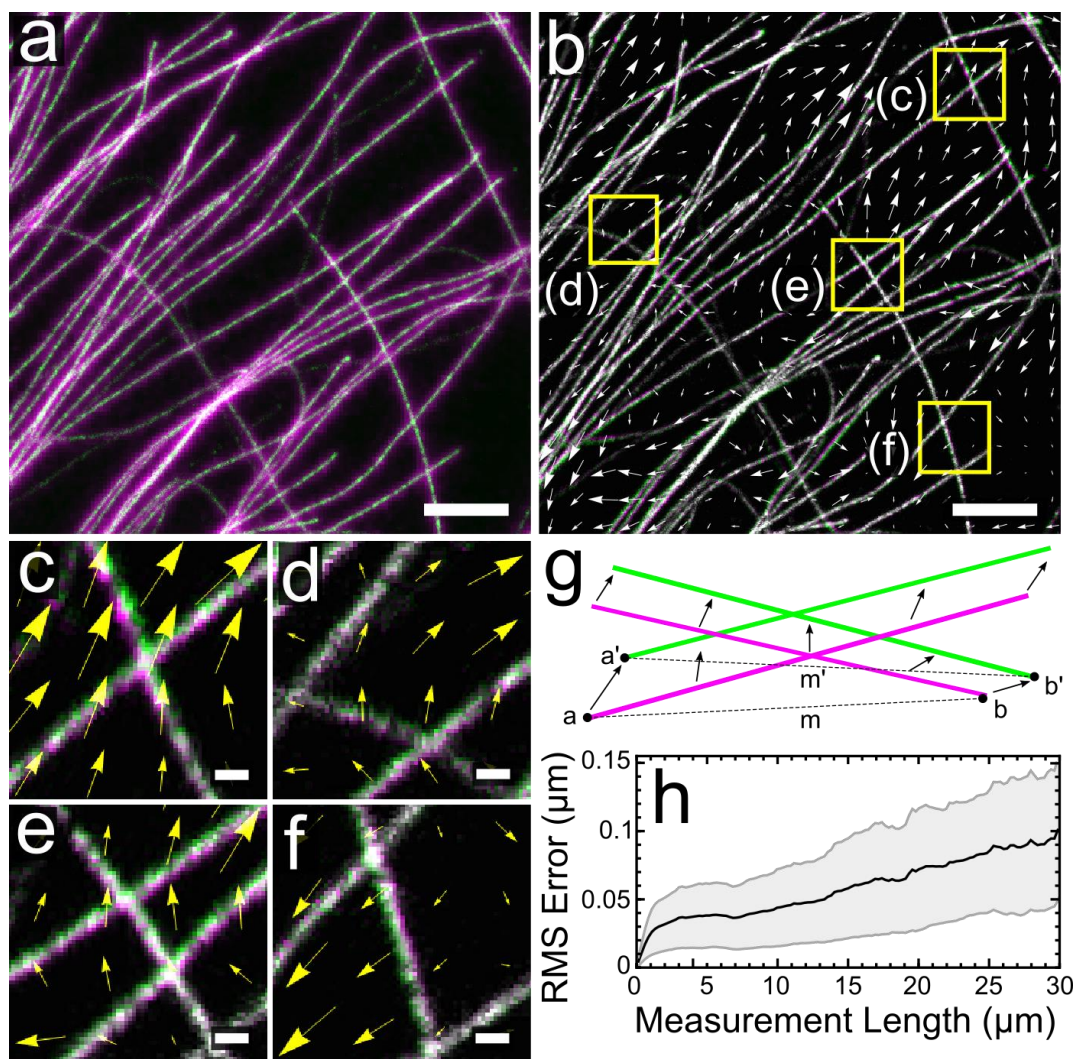


**Supplementary Figure 1.** Epifluorescence images of expanded BS-C-1 cells that were immunostained against tubulin using conventional fluorophore-labeled antibodies and then treated as indicated prior to gelation, digestion, and expansion. **(a)** Omission of post-stain treatment leads to heavy distortion due to lack of retention along the original structure. Post-stain treatment of immunostained cells with **(b)** MA-NHS (methacrylic acid *N*-hydroxyl succinimidyl ester) or **(c)** GA (glutaraldehyde) both conferred excellent retention of fluorescence and structure. Scale bars are 2.4  $\mu\text{m}$  and are all in pre-expansion dimensions.



**Supplementary Figure 2.** Confocal fluorescence measurement of microtubule cross-sectional profile for 4.15 $\times$  expanded specimens and estimate of spatial resolution. **(a)** Confocal fluorescence image of an expanded BS-C-1 cell conventionally immunostained for tyrosinated tubulin and treated with GA prior to gelation. **(b)** Representative cross-sectional profiles of microtubules (red lines) and Gaussian fits (dashed black lines). **(c)** Analysis of microtubule profiles (red lines in **a**) yielded an average Gaussian-fitted full width at half maximum (FWHM) of  $79 \pm 9$  nm (mean  $\pm$  SD, 362 microtubule profiles). **(d-f)** Cross-sectional profile analysis for an expanded, MA-NHS treated, conventionally immunostained BS-C-1 cell showing an average FWHM of  $80 \pm 7$  nm (mean  $\pm$  SD, 353 microtubule profiles). All distances and scale bars correspond to pre-expansion dimensions. Scale bars are 5  $\mu$ m.

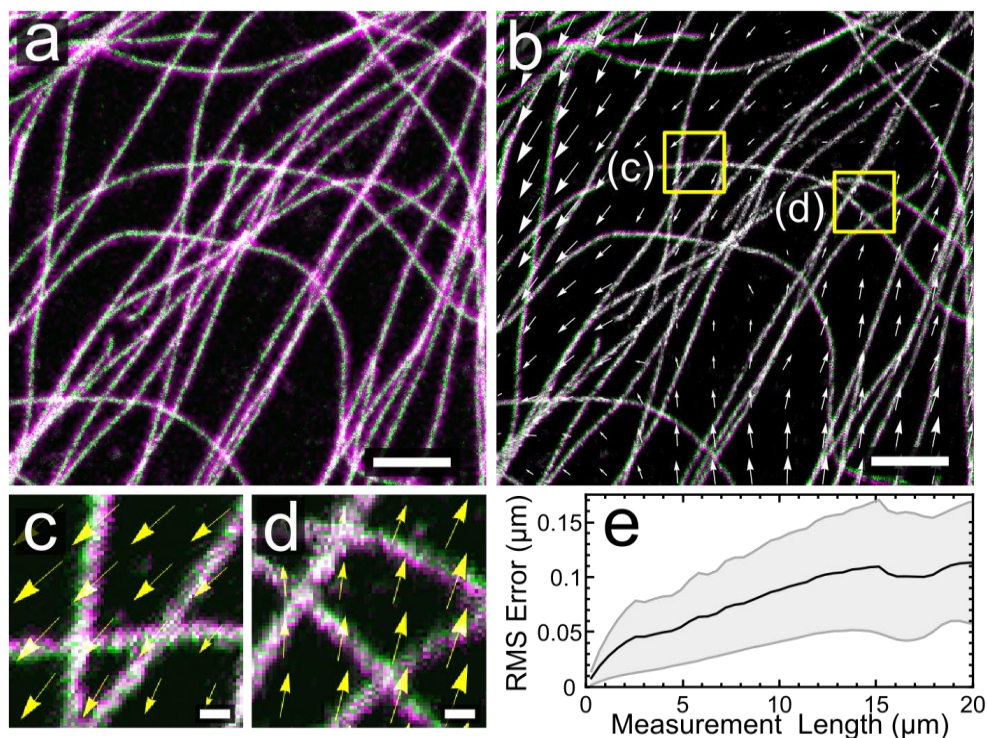
*Resolution estimate:* The observed  $\sim 80$  nm FWHM profile of microtubules is consistent with the convolution of the double-peaked spatial profile of indirectly immunostained microtubules (measured by localization microscopy at  $\sim 20$  nm resolution, **Supplementary Fig. 5**) with an effective  $\sim 65$  nm Gaussian point spread function (PSF) for expansion microscopy. The value of 65 nm is also approximately equal to the physical PSF of our microscope ( $\sim 265$  nm FWHM, when configured with the 63 $\times$  1.2NA water-immersion lens used here) divided by the measured expansion factor of 4.15.



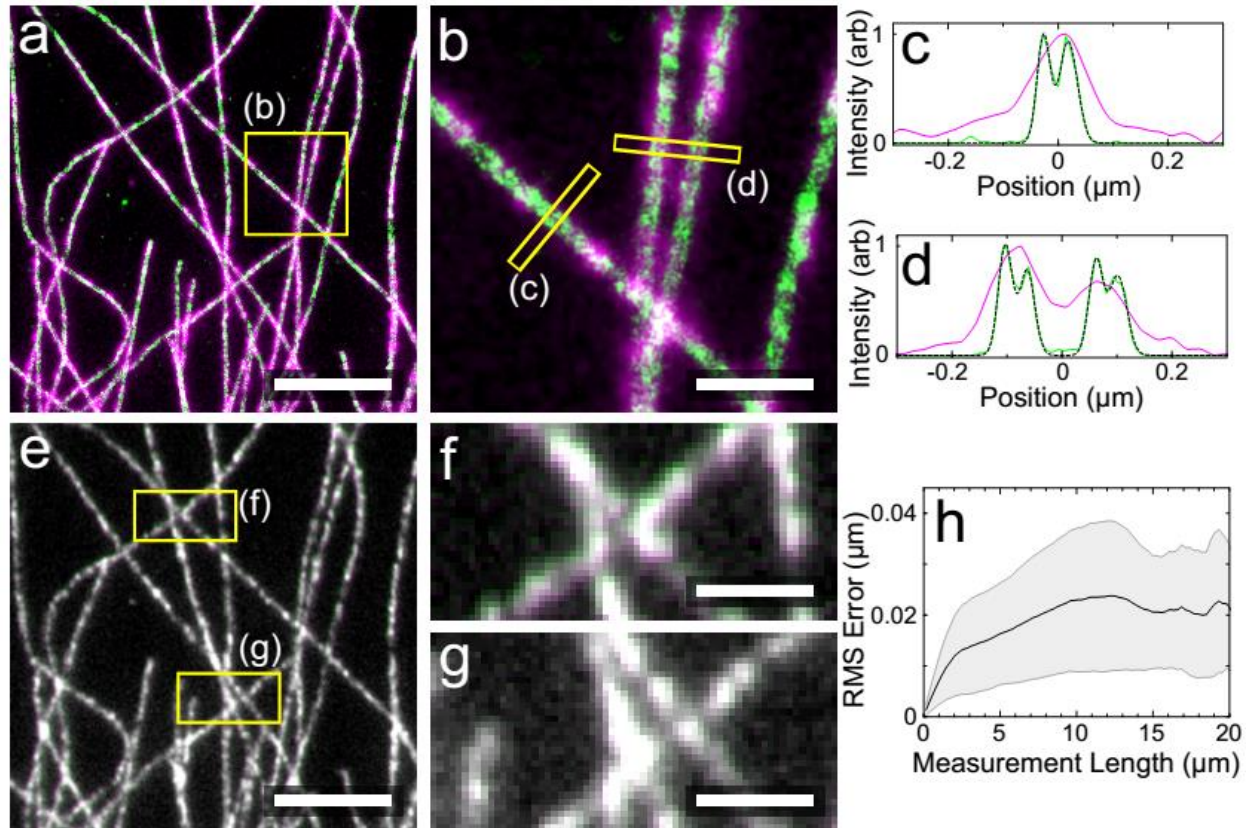
**Supplementary Figure 3.** Comparison of pre-expansion and post-expansion images recorded by confocal fluorescence microscopy for a region of a BS-C-1 cell immunostained for tyrosinated tubulin with a conventional Atto 488 secondary antibody and treated with MA-NHS before gelation (data from **Fig. 2**). **(a)** Overlay of pre-expansion image (magenta) and post-expansion image (green) after alignment of the post-expansion image using similarity registration (i.e., translation, rotation, and magnification—see methods for further details). **(b)** Overlay of post-expansion image before (magenta) and after (green) a non-rigid transformation procedure that uses B-spline registration to “warp” the post-expansion image to optimally fit the pre-expansion image. Arrows indicate the direction and relative magnitude (scaled 8×) of the transformation required to optimally align the post-expansion to the pre-expansion image. **(c–f)** Zoom-in images of boxed regions in **b** showing that distortions are generally very small. **(g)** Schematic of procedure used to measure distances  $m$  and  $m'$  between features  $a$  and  $b$  in the post-B-spline-registration (green) and corresponding features  $a'$  and  $b'$  in pre-B-spline-registration (magenta). **(h)** Quantification of root mean square (RMS) error of  $m-m'$  as a

function of distance  $m$  for matching image features (black line) with plus or minus standard deviation. The plot in **h** was calculated from a  $20\ \mu\text{m} \times 20\ \mu\text{m}$  data set; the image in **a** shows a  $12\ \mu\text{m} \times 12\ \mu\text{m}$  zoom-in of the data set. All distances and scale bars correspond to pre-expansion dimensions. Scale bars (**a, b**)  $2\ \mu\text{m}$ , (**c-f**)  $200\ \text{nm}$ .



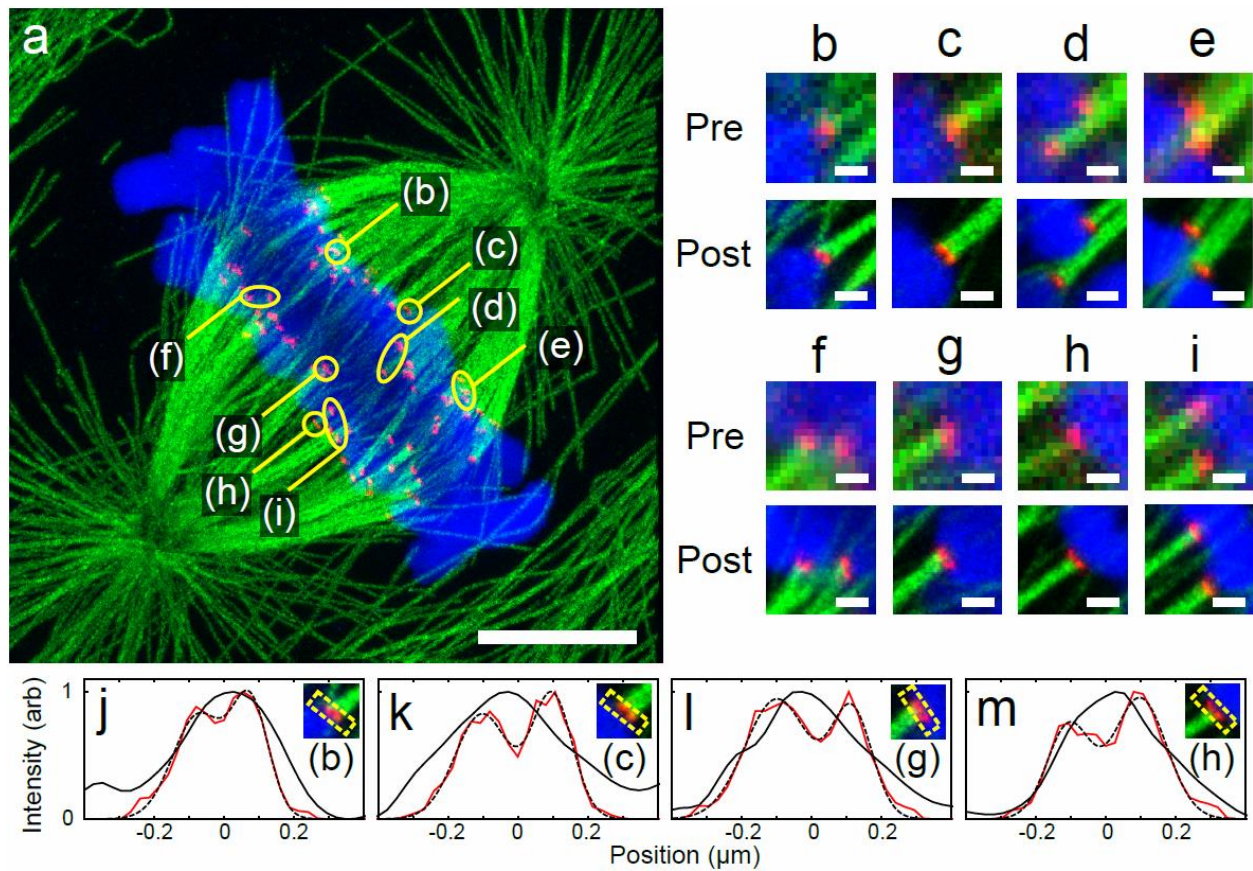


**Supplementary Figure 4.** Comparison of pre-expansion and post-expansion images recorded by confocal fluorescence microscopy for a region of a BS-C-1 cell immunostained for tubulin with DNA-labeled secondary antibodies and hybridized with a modified complementary strand (5' acrydite and 3' Atto 488) prior to gelation. **(a)** Overlay of pre-expansion image (magenta) and post-expansion image (green) after alignment of the post-expansion image using similarity registration. **(b)** Overlay of post-expansion image before (magenta) and after (green) using a non-rigid B-spline registration. Arrows indicate the direction and relative magnitude (scaled 8x) of the transformation required to optimally align the images. **(c,d)** Zoom-in images of boxed regions in **b** showing that distortions are generally very small. **(e)** RMS error vs length distortion analysis for data in **a** (see **Supplementary Fig. 3**). The plot in **e** was calculated from a 20  $\mu\text{m} \times 20 \mu\text{m}$  data set; the image in **a** shows a 12  $\mu\text{m} \times 12 \mu\text{m}$  zoom-in of the data set. All distances and scale bars correspond to pre-expansion dimensions. Scale bars **(a, b)** 2  $\mu\text{m}$ , **(c,d)** 200 nm.

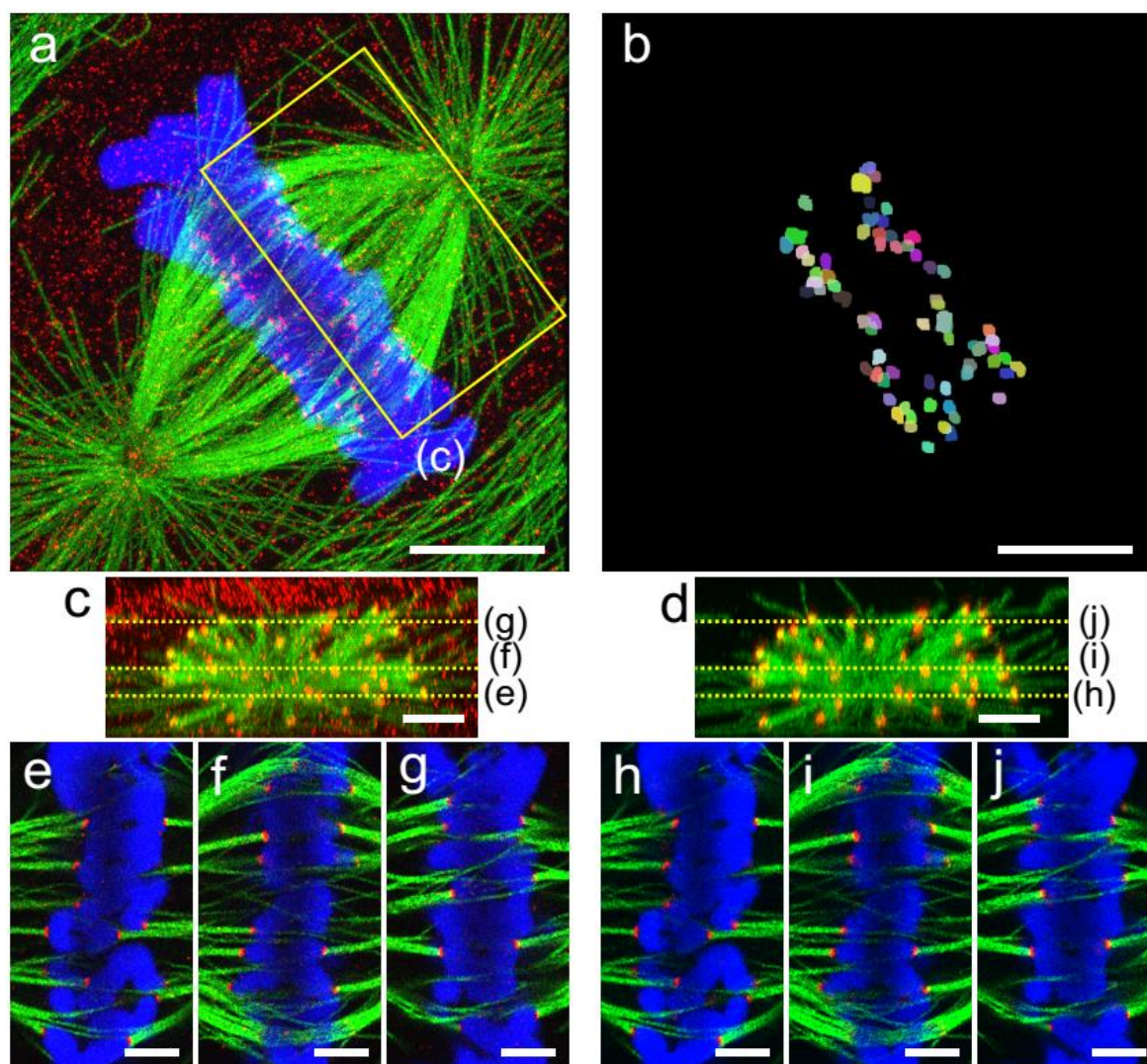


**Supplementary Figure 5.** Comparison of pre-expansion image measured by localization microscopy and post-expansion image measured by epifluorescence microscopy for a BS-C-1 cell immunostained with conventional antibodies and treated with GA prior to gelation. **(a)** Overlay of pre-expansion image (green) and post-expansion image (magenta) after alignment of the post-expansion image using similarity registration. **(b)** Zoom-in of boxed region in **a** showing close agreement between localization microscopy image and expansion microscopy image. **(c, d)** Line profiles of the boxed regions in **b**. **(e)** Overlay of post-expansion image before (magenta) and after (green) B-spline registration as described in **Supplementary Fig. 3**. **(f-g)** Zoom-in images from boxed regions in **e** showing that distortions are generally very small. **(h)** RMS error vs length distortion analysis for data in **a** (see **Supplementary Fig. 3**). The plot in **h** was calculated from a  $20\ \mu\text{m} \times 20\ \mu\text{m}$  data set; the image in **a** shows an  $8\ \mu\text{m} \times 8\ \mu\text{m}$  zoom-in of the data set. All distances and scale bars correspond to pre-expansion dimensions. Scale bars, **(a, e)**  $2\ \mu\text{m}$ , **(b)**  $500\ \text{nm}$ , **(f, g)**  $250\ \text{nm}$ .



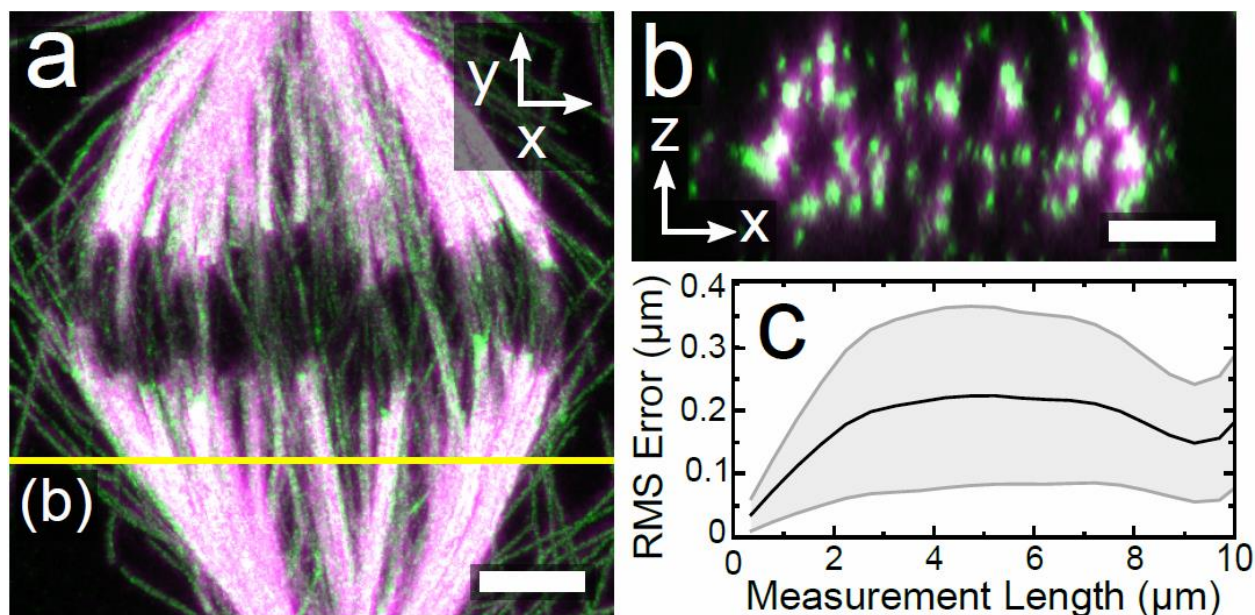


**Supplementary Figure 6.** Comparison of attachments of kinetochore fibers (K-fibers) and chromosomes for mitotic cell from **Fig. 2 e-j**. **(a)** Maximum intensity projection of a post-expansion image of a dividing PtK1 cell that was immunostained against tyrosinated tubulin (green) and HEC1 (red) using conventional Atto 488 and dually labeled Alexa Fluor 546 and biotin secondary antibodies, respectively, and stained for DNA using TO-PRO-3 (blue). **(b-i)** Comparison of pre-expansion images of kinetochore attachments with corresponding post-expansion images, both imaged by confocal microscopy in z-sections from 400-800 nm thickness. **(j-m)** A subset of attachments showed double-peaked signals that were not resolvable in the pre-expansion images. Cross-sectional profiles of HEC1 signal from **b**, **c**, **g**, and **h**, for pre-expansion images (solid black), post-expansion images (red), and a double-Gaussian fit to the post-expansion signals (dashed black lines). Double peaks are separated by 149 nm, 201 nm, 214 nm, and 204 nm, respectively. All distances and scale bars correspond to pre-expansion dimensions. Scale bars, **(a)** 5  $\mu\text{m}$ , **(b-i)** 500 nm.

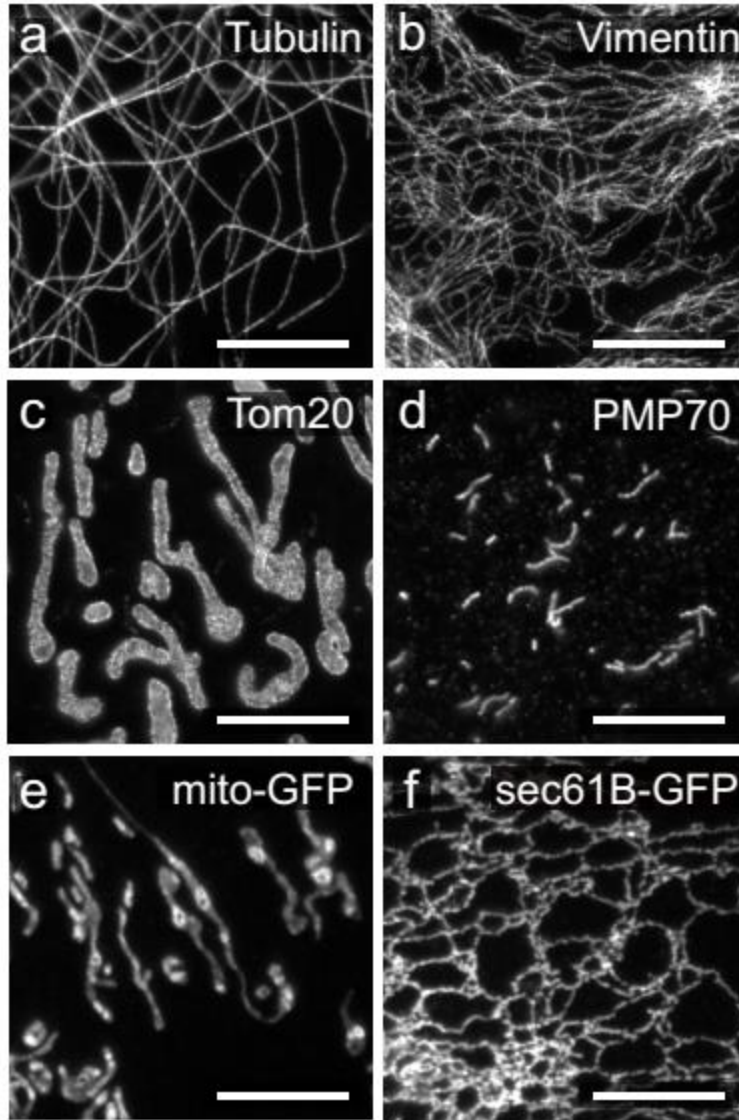


**Supplementary Figure 7.** Image processing on post-expansion mitotic spindle data. Unprocessed confocal maximum intensity projection (**a**) of mitotic cell from **Fig. 2** and binarized kinetochore mask (**b**) resulting from image filtering (see **methods** for additional details). Cross-sectional maximum intensity projection of boxed area in **a** showing non-specific adsorption of the HEC1 antibody (red) to the cell periphery (**c**) and processed cross-section (**d**). Unprocessed (**e-g**) versus processed (**h-j**) single z-section (~225 nm thickness) showing that kinetochore attachments are retained after processing. All distances and scale bars correspond to pre-expansion dimensions. Scale bars, (**a**, **b**) 5  $\mu\text{m}$ , (**c-j**) 2  $\mu\text{m}$ .

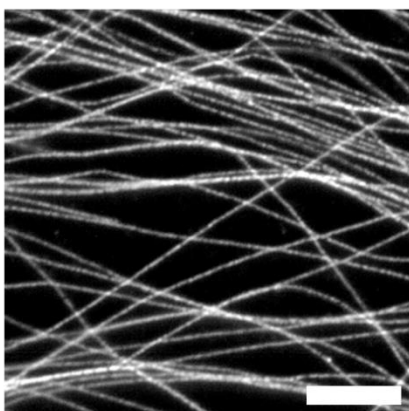
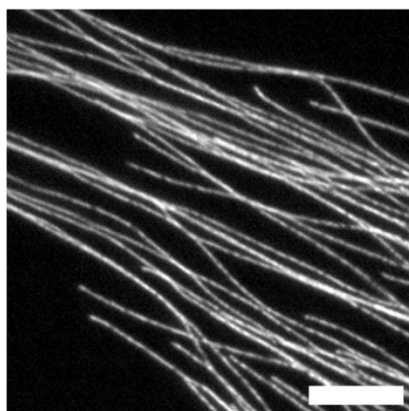
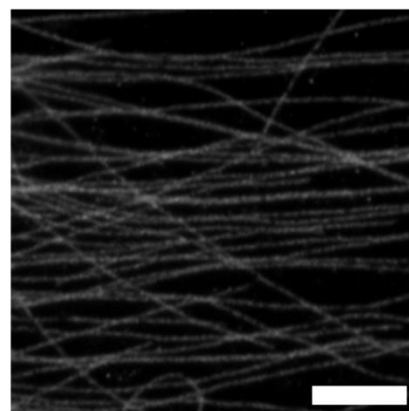




**Supplementary Figure 8.** Comparison of pre-expansion and post-expansion images recorded by confocal fluorescence microscopy for immunostained mitotic PtK1 cell (data from **Fig. 2**, only tubulin channel). **(a)** XY maximum intensity projection overlay of pre-expansion (magenta) and post-expansion (green) images after alignment using three-dimensional similarity registration. **(b)** XZ maximum intensity projection along yellow line in **a**. **(c)** RMS error vs length distortion analysis in three dimensions (see **Supplementary Fig. 3**). Scale bars  $2\ \mu\text{m}$ . All distances and scale bars correspond to pre-expansion dimensions.

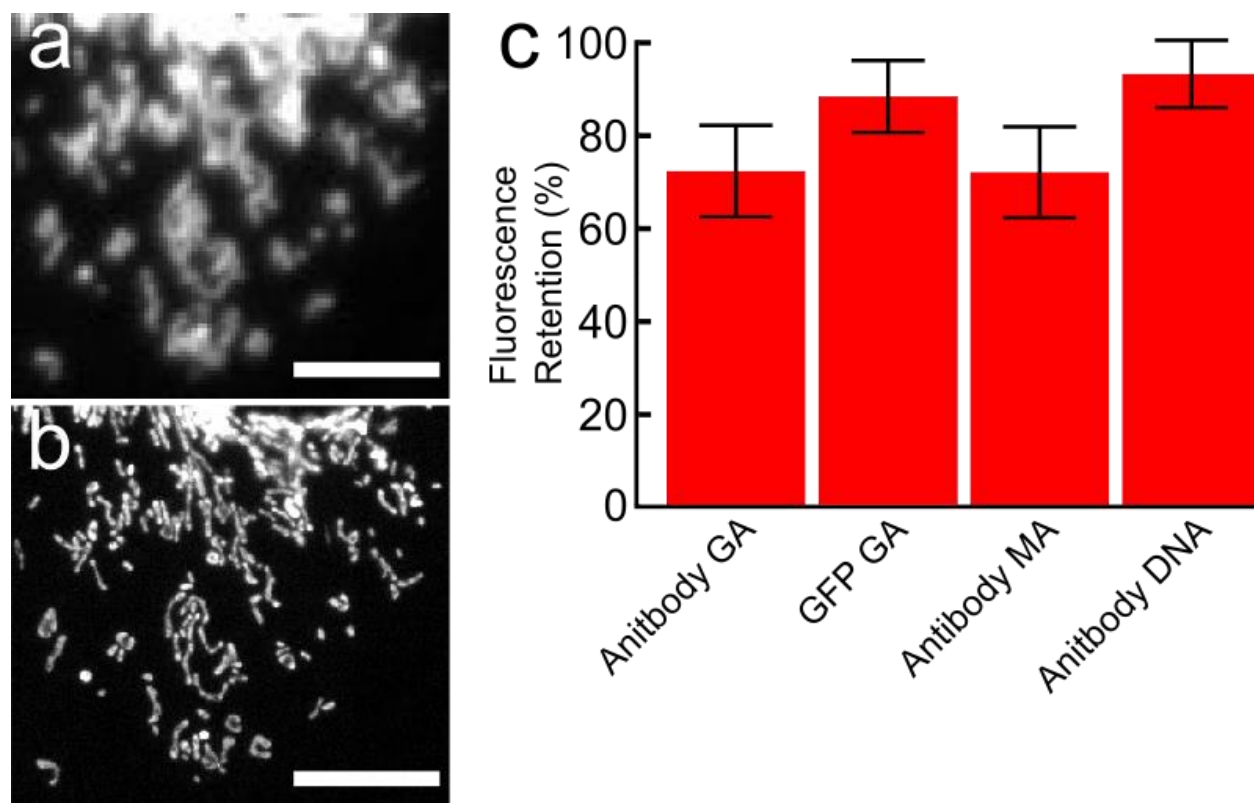


**Supplementary Figure 9.** Gallery of expanded cellular structures. Epifluorescence images of expanded BS-C-1 cells indirectly immunostained with Atto 488 against **(a)** tyrosinated tubulin, **(b)** vimentin, **(c)** TOM20 (outer mitochondrial membrane), **(d)** PMP70 (peroxisomal membrane protein), **(e)** mito-GFP (inner mitochondrial membrane marker) and **(f)** Sec61 $\beta$ -GFP (endoplasmic reticulum marker) and treated with GA. Scale bars are 4.8  $\mu$ m and are all in pre-expansion dimensions.

**a) GA treatment****b) MA treatment****c) DNA antibody**

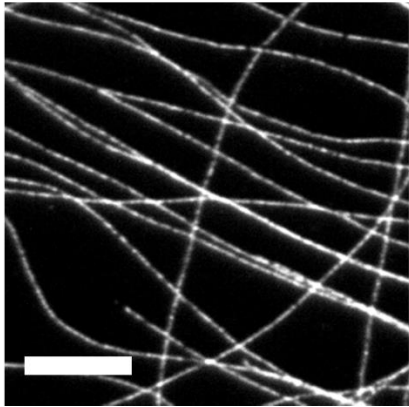
**Supplementary Figure 10.** Epifluorescence images of expanded BS-C-1 cells stained for tyrosinated tubulin using different procedures. In (a), fixed cells were immunostained using conventional fluorescently-labeled antibodies and then treated with GA. In (b), fixed cells were immunostained using conventional fluorescently-labeled antibodies and then treated MA-NHS prior to gelation. In (c), fixed cells were immunostained using DNA-labeled antibodies which we prepared according to the protocol published by Boyden and coworkers.<sup>1</sup> Image contrasts have been matched to show the relative brightness of the stain achieved in each case; the specimens treated with MA-NHS or GA were both approximately 3-4 times brighter than that of the specimen stained using the DNA-labeled antibody. We note that the number of fluorophores per antibody with the DNA-labeled antibodies was not reported in the original expansion publication and it is possible that an optimized DNA-labeled antibody could be brighter than the one we prepared here.<sup>1</sup> However, we believe the DNA-labeled antibodies would be unlikely to achieve brighter stains than conventional (directly) fluorescently-labeled antibodies due to the more than ten-fold difference in molecular weight between an individual fluorophore and a 20-mer single-stranded oligonucleotide. Scale bars are 2.4  $\mu\text{m}$  and are all in pre-expansion dimensions.



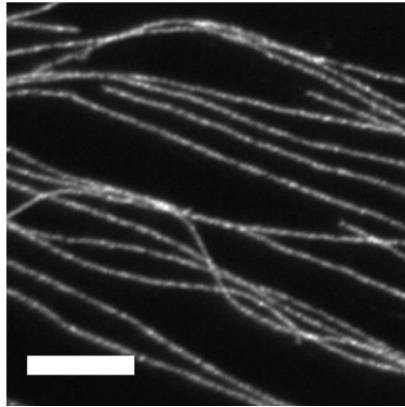


**Supplementary Figure 11.** Determination of fluorescence retention for each method performed in this work using epifluorescence imaging. In each case, the total fluorescence of individual mitochondria was measured before and after expansion using a 20× 0.45 NA air objective. Fluorescence retention of GFP was measured using the inner mitochondrial membrane tag mito-GFP while all other methods used an outer mitochondria immunostain for TOM20 using Atto 488. **(a)** Pre-expansion image of a representative area used in the determination of GFP fluorescence retention. **(b)** Corresponding area in **a** after expansion. Scale bars are 10  $\mu$ m in pre-expansion dimensions. **(c)** Bar graph of fluorescence retention for each method used in this work. Error bars represent the standard deviation in measured fluorescence retention (n=20).

**a) Home-made AB**

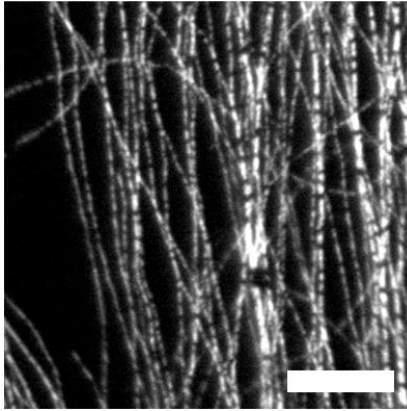


**b) Commercial AB**

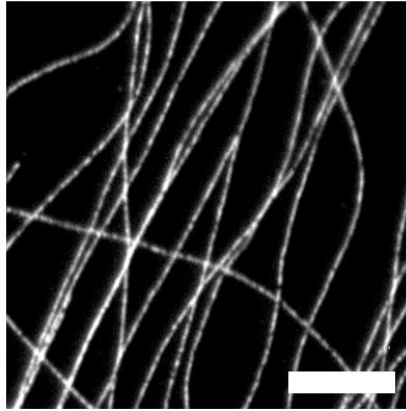


**Supplementary Figure 12.** Epifluorescence images of expanded BS-C-1 cells prepared using the GA treatment method. Cells were indirectly immunostained for tyrosinated tubulin using either a homemade Atto 488 donkey anti-rat secondary antibody (**a**) or a commercially available Alexa Fluor 488 donkey anti-rat secondary antibody (**b**). Image contrasts were adjusted to be proportional to exposure time in order to show that the two stains are comparable in brightness. Scale bars are 2.4  $\mu\text{m}$  and are all in pre-expansion dimensions.

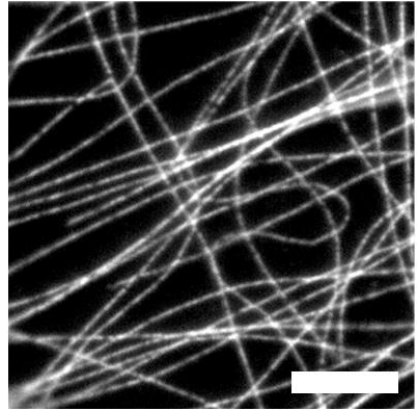
**a) 0 min**



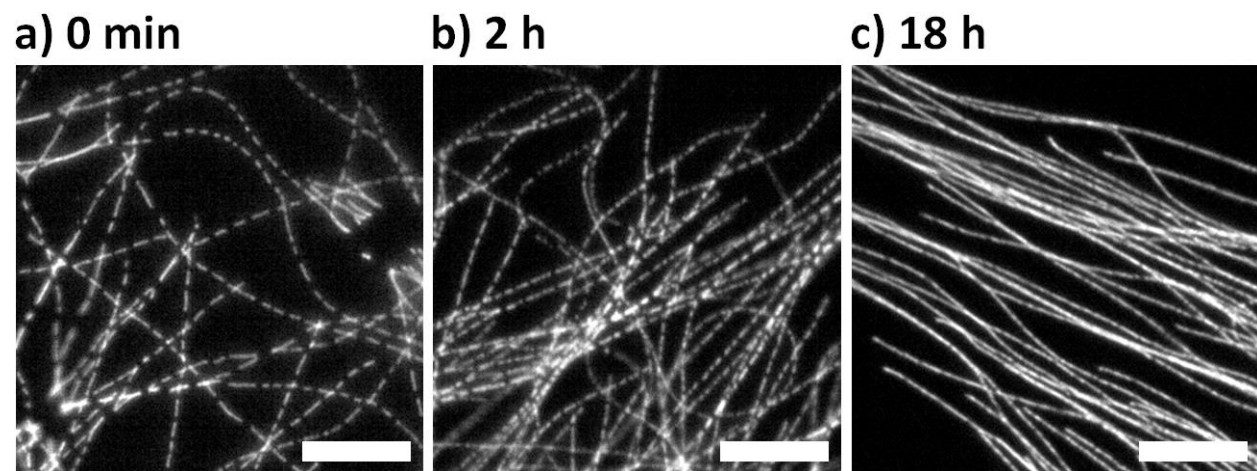
**b) 30 min**



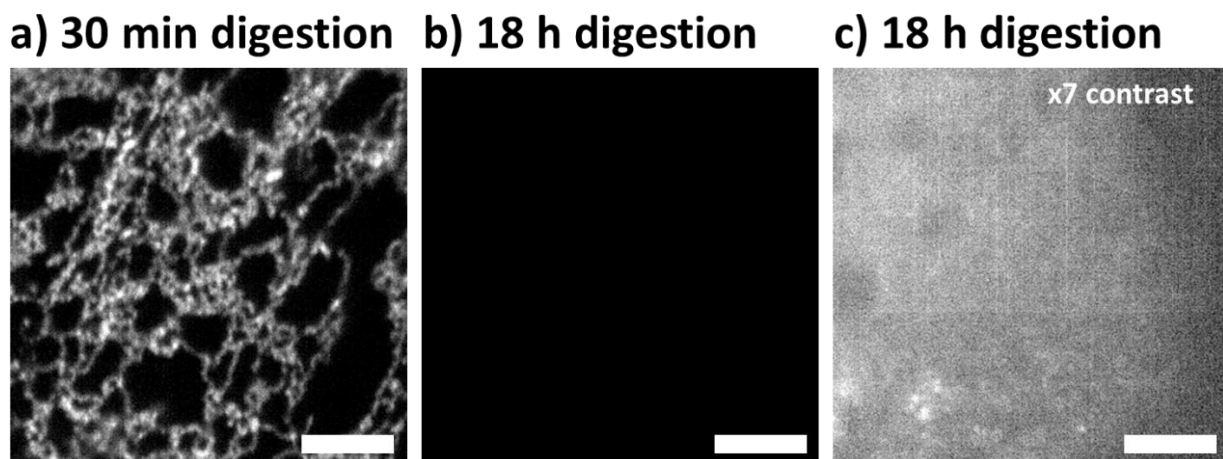
**c) 18 h**



**Supplementary Figure 13.** (a-c) Epifluorescence images of expanded BS-C-1 cells stained for tyrosinated tubulin, treated with GA, and digested for the period indicated. Digestion times shorter than 30 minutes show prominent distortions while these are largely absent for digestion times of 30 minutes or longer. Scale bars are 2.4  $\mu\text{m}$  and are all in pre-expansion dimensions.

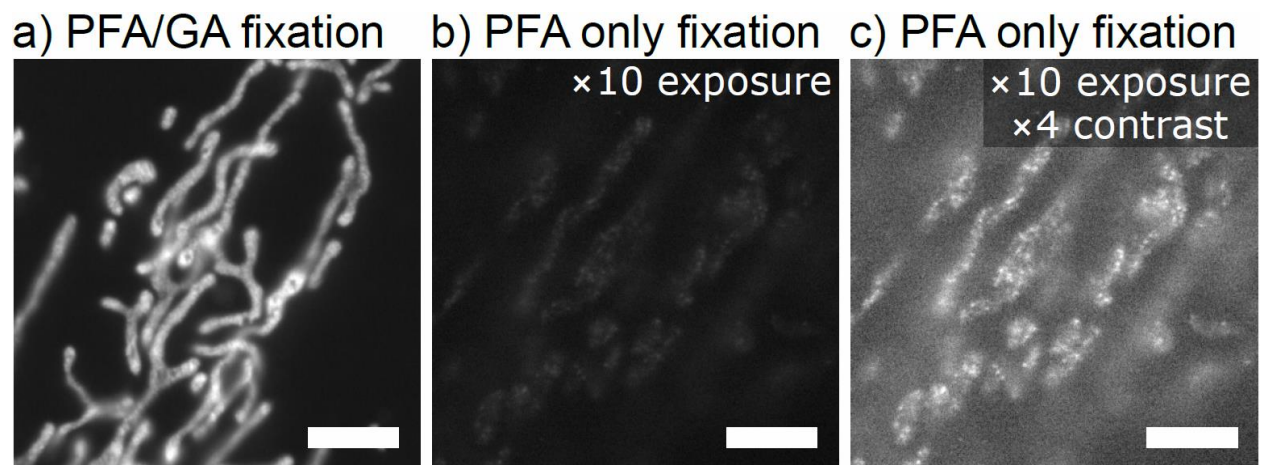


**Supplementary Figure 14.** (a-c) Epifluorescence images of expanded BS-C-1 cells stained for tyrosinated tubulin, treated with MA-NHS, and digested for the period indicated. Digestion times of many hours were required to avoid prominent distortions. Scale bars are 2.4  $\mu\text{m}$  and are all in pre-expansion dimensions.



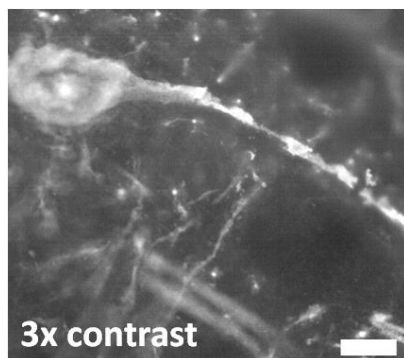
**Supplementary Figure 15.** Epifluorescence images of expanded BS-C-1 cells expressing Sec61 $\beta$ -GFP and treated with GA during fixation; intrinsic GFP signal is only retained for short digestion times in cultured cells. In **(a)**, the sample was digested for 30 min. In **(b)**, the sample was digested for 18 h. The images in **a** and **b** were acquired under identical illumination conditions, exposure durations, and are displayed with the same contrast. Panel **(c)** is the same image as in **b** but with 7 $\times$  contrast to show weak residual fluorescence. Scale bars are 2.4  $\mu$ m and are all in pre-expansion dimensions.



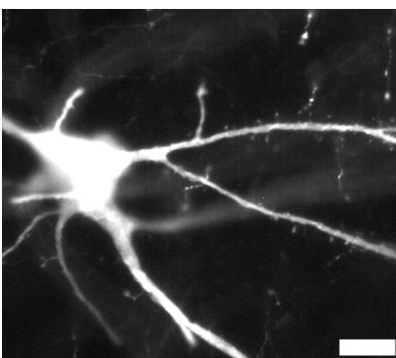


**Supplementary Figure 16.** Epifluorescence images of expanded BS-C-1 cells expressing mito-GFP and digested for 30 minutes; intrinsic GFP signal is only retained for GA-treated cells. **a)** Treatment with a mixture of PFA/GA (paraformaldehyde and glutaraldehyde) during fixation retains intrinsic fluorescence from mito-GFP, whereas **b)** treatment with only PFA does not. Both specimens were subjected to a digestion time of 30 min. Panels **a** and **b** are displayed at the same contrast although panel **b** was recorded with ten times the exposure duration. **c)** Adjustment of the contrast of the image in **b** allows observation of dim residual signal. Scale bars are 2.4  $\mu\text{m}$  and are all in pre-expansion dimensions.

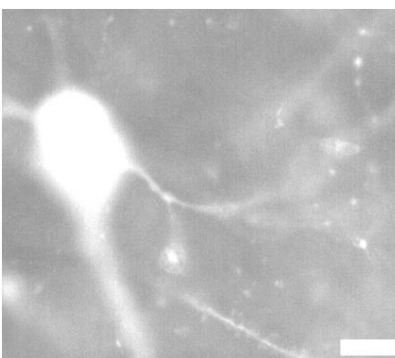
**a) No treatment**



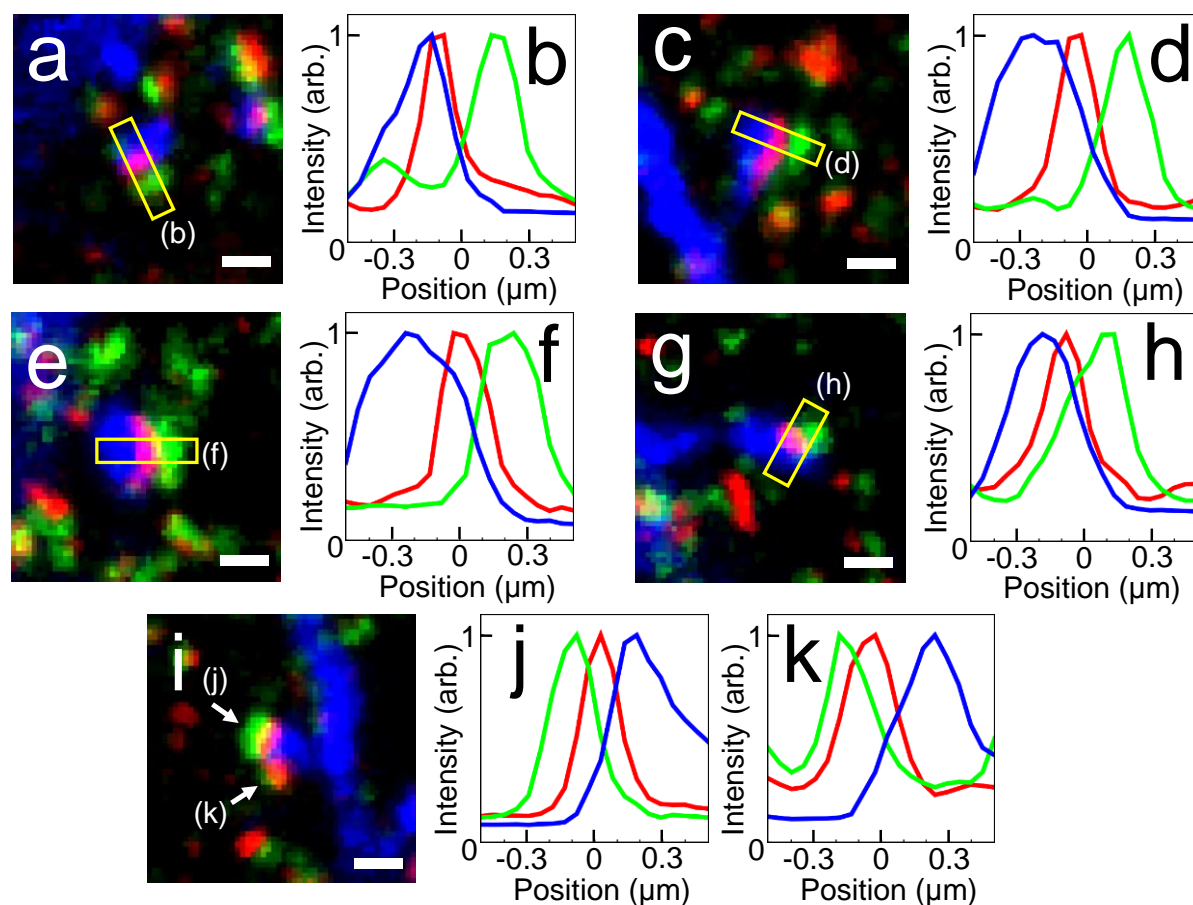
**b) MA-NHS treatment**



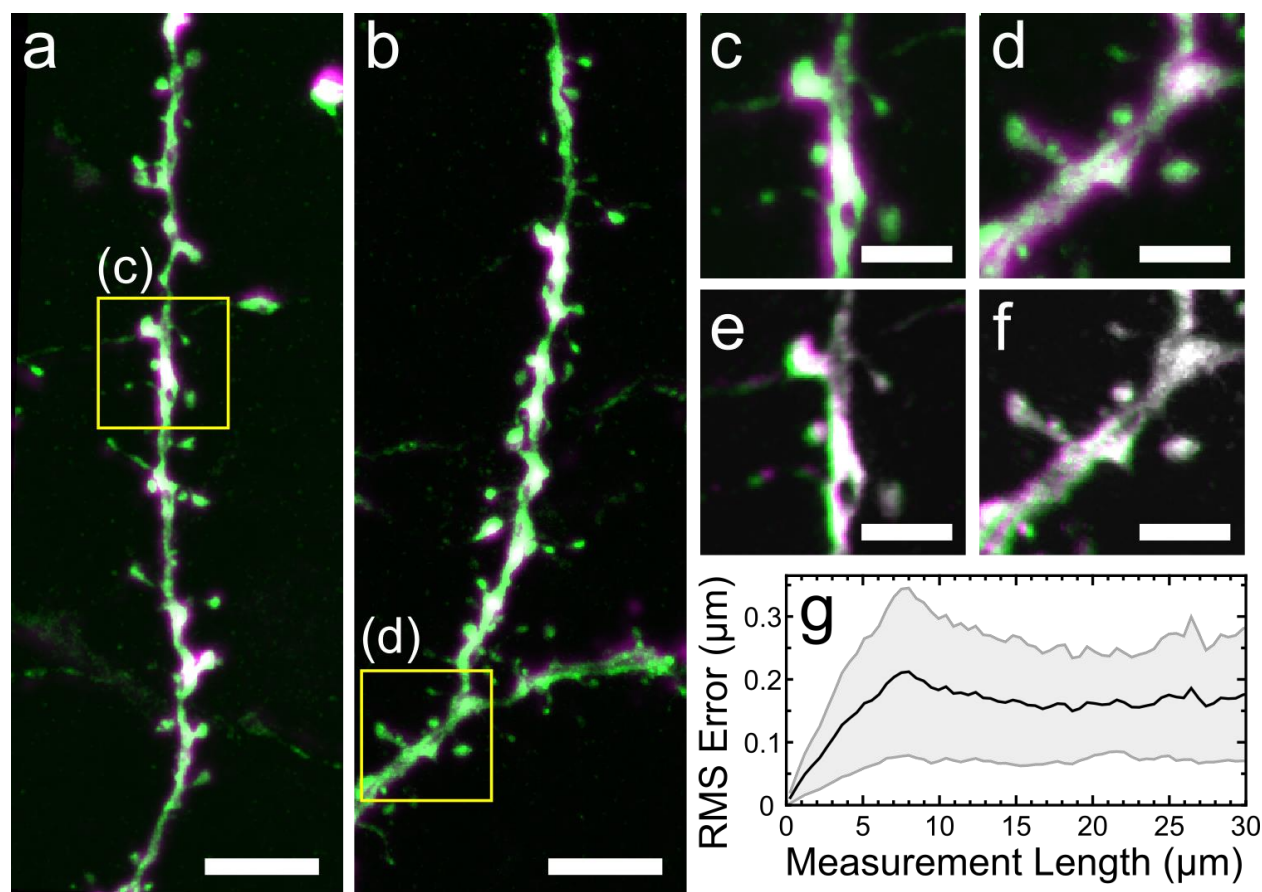
**c) GA treatment**



**Supplementary Figure 17.** Epifluorescence images of expanded 100  $\mu\text{m}$  thick THY1-YFP-H mouse brain slices immunostained for YFP and subjected to various post-stain treatments. **(a)** No treatment leads to low signal intensity and patchy preservation of signal along structure. **(b)** Treatment with MA-NHS after immunostaining led to higher signal levels with good retention along the original structures. **(c)** Treatment with GA after immunostaining resulted in high background signal. The three images were acquired using identical illumination and exposure; the images in **b** and **c** are displayed at the same contrast, while **a** is displayed with 3 $\times$  contrast to show details within the comparably dim image. Due to the comparably long ( $\sim 12$  hour) digestion used here, there should be a negligibly small amount of intrinsic YFP signal remaining, in comparison to the data in **Supplementary Fig. 20** which show weak residual YFP signal after a 60 min digestion. Scale bars are 12  $\mu\text{m}$  and are all in pre-expansion dimensions.

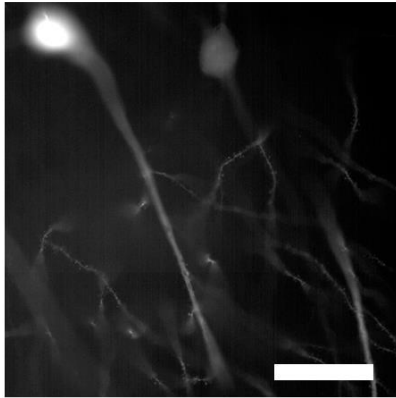


**Supplementary Figure 18.** Gallery of expanded synapses in mouse brain tissue. Maximum intensity projections (**a, c, e, g, i**) of expanded THY1-YFP-H mouse brain tissue indirectly immunostained for YFP (blue, Atto 488), Bassoon (green, Atto 565), and Homer (red, Atto 647N) along with corresponding cross-sectional profiles of the indicated individual synapses (**b, d, f, h, j, k**). In each case, the pre- and postsynaptic densities are clearly resolvable and align well with dendritic spines. In **i**, two separate synapses are shown connecting to a single dendritic spine (cross-sectional profiles indicated with arrows). All distances and scale bars correspond to pre-expansion dimensions. Scale bars are 500 nm.

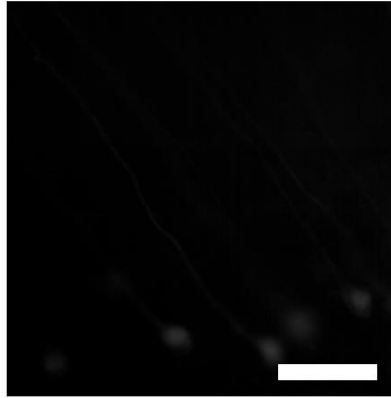


**Supplementary Figure 19.** Comparison of pre-expansion and post-expansion images recorded by confocal fluorescence microscopy for a 100  $\mu\text{m}$  thick THY1-YFP-H mouse brain slices immunostained for YFP. **(a, b)** Large area overlay of pre-expansion image (magenta) and post-expansion image (green) after alignment of the post-expansion image using similarity registration. **(c, d)** Overlay pre-expansion image (magenta) and post-expansion image (green) using similarity transformation in a local region. **(e, f)** Overlay of post-expansion images from before (magenta) and after (green) B-spline registration as described in **Supplementary Fig. 3**. **(g)** RMS error vs length distortion analysis for data in **a** and **b** (see **Supplementary Fig. 3**). All distances and scale bars correspond to pre-expansion dimensions. Scale bars **(a, b)** 10  $\mu\text{m}$ , **(c, d, e, f)** 5  $\mu\text{m}$ .

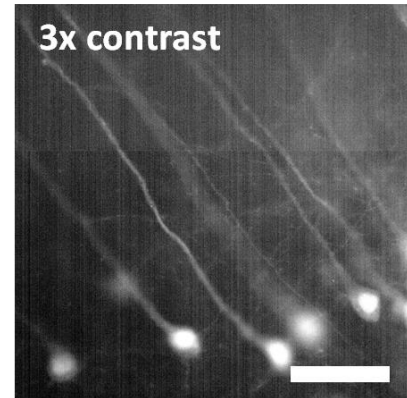
**a) MA-NHS treatment**



**b) No treatment**

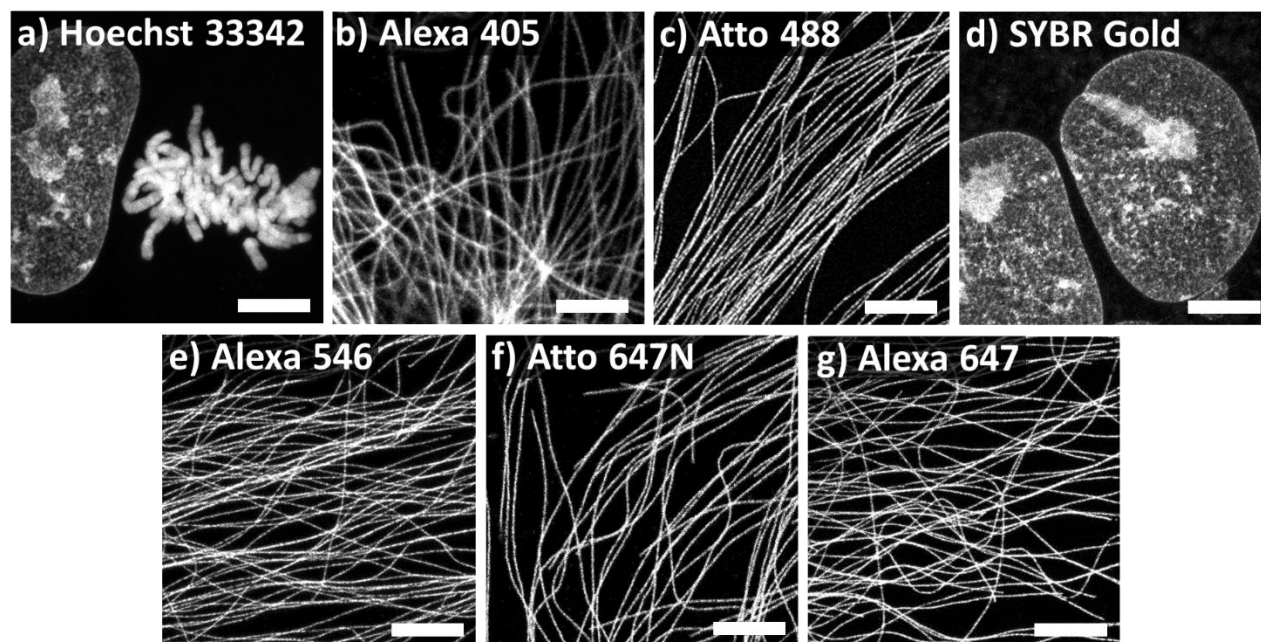


**c) No treatment**



**Supplementary Figure 20.** Epifluorescence images of 100  $\mu\text{m}$  thick THY1-YFP-H mouse brain slices treated with either MA-NHS or nothing prior to gelation, a brief (60 min) digestion, and expansion. While both specimens expanded well, the MA-NHS treated brain slice in **(a)** showed much higher intrinsic YFP signal than the non-treated brain slice shown in **(b)**. The images in **a** and **b** were acquired with identical illumination and exposure and are displayed with the same contrast settings. The image in **(c)** is a duplicate of that in **b** but is displayed with 3x contrast. Note that use of a long digestion time (>12 hours) led to essentially zero detectable signal (data not shown). Scale bars are 30  $\mu\text{m}$  (pre-expansion dimensions).





**Supplementary Figure 21.** Confocal fluorescence maximum intensity projections of expanded BS-C-1 cells stained for DNA or immunostained against tyrosinated tubulin using various secondary antibodies and treated with GA prior to gelation. In panels **b**, **c**, **e**, and **f**, conventional secondary antibodies were used that were directly labeled with the indicated fluorophore. Panels **a** and **d** were stained for nuclear DNA using the corresponding dye without subsequent GA treatment. In **g**, a biotinylated secondary antibody was used prior to treatment with GA; after expansion the sample was incubated with Alexa Fluor 647 labeled streptavidin. Post-expansion labeling offers a way to introduce fluorophores to the sample that would otherwise not survive the polymerization step such as Alexa Fluor 647 and other cyanines.<sup>1</sup> Scale bars are 3.75  $\mu\text{m}$  and are all in pre-expansion dimensions.

**Supplementary Video 1.** 3D animation of expanded brain slice shown in **Fig. 3**. The animation begins as  $29 \times 13 \mu\text{m}$  and then zooms to show a view of  $4.6 \times 2.7 \mu\text{m}$  (all distances are in pre-expansion dimensions).

**Supplementary Table 1. Summary of sample preparation and imaging conditions.**

Figure	Specimen	Fixation	1° Ab all 1-2 µg/mL	2° Ab, etc., & dyes/protein 1-2.5 µg/mL, except as indicated	Polymer-linking	Digestion time & other notes	Imaging Image thicknesses in pre- expansion dimensions
<b>2 a-c</b>	BS-C-1 cell, wildtype	Extracted, then PFA/GA	Rat × Tub & Rb × dTub	D × Rat Atto 488 (~5.6 d/p) & D × Rb Alexa 546 (~12 d/p)	25 mM MA-NHS, 60 min	Overnight	Confocal, 63× 1.2NA water lens. Image thicknesses: <b>a)</b> 900/200 nm; <b>b)</b> 900 nm; <b>c)</b> 225 nm
<b>2 e-j,</b> <b>Supp.</b> <b>Fig. 6,</b> <b>7, 8</b>	PtK1 cell, wildtype	Extracted, then PFA/GA	Rat × Tub & Ms × HEC1	D × Rat Atto 488 (~7.1 d/p) & D × Ms Alexa 546 (~5 d/p) +biotin	0.25% GA 10 min	Overnight digestion; post- expansion incubation with streptavidin Alexa 546 (2 µg/mL, ~7 d/p) and TO-PRO-3 (1 µM)	Confocal, 63× 1.2NA water lens. Image thicknesses: <b>2e,f)</b> 5.6 µm; <b>2g)</b> 900 nm; <b>2h)</b> 420 nm; <b>56)</b> ~800 nm; <b>57a)</b> 5.6 µm; <b>57e-j)</b> 225 nm; <b>58a)</b> 5.6 µm; <b>58b)</b> 130 nm.
<b>2 k-l</b>	BS-C-1 cell expressing Sec61β-GFP & mito- DsRed	PFA/GA, 37 °C	Rb × TOM20	D × Rb Atto 647 N (~2.7 d/p)	0.25% GA 10 min	30 min	Confocal, 63× 1.2NA water lens. Detected intrinsic GFP & YFP signal as well as signal from Atto 647N stain. Image thicknesses: <b>k)</b> 1 µm; <b>l)</b> 225 nm
<b>Supp.</b> <b>Fig. 1</b>	BS-C-1 cells, wildtype	Extracted, then PFA/GA	Rat × Tub	D × Rb Atto 488 (9-12 d/p)	<b>a)</b> no treatment <b>b)</b> 25 mM MA-NHS 60 min <b>c)</b> 0.25% GA 10 min	Overnight	Epifluorescence, 60× 1.2NA water lens
<b>Supp.</b> <b>Fig. 2</b>	BS-C-1 cells, wildtype	Extracted, then PFA/GA	Rat × Tub	D × Rat Atto 488 (~5.6 d/p)	<b>a)</b> 0.25% GA 10 min <b>c)</b> 25 mM MA-NHS 60 min	Overnight	Confocal, 63× 1.2NA water lens. Image thickness ~225 nm
<b>Supp.</b> <b>Fig. 3</b>	BS-C-1 cell, wildtype	Extracted, then PFA/GA	Rat × Tub	D × Rat Atto 488 (~5.6 d/p)	25 mM MA-NHS, 60 min	Overnight	Confocal, 63× 1.2 NA water lens. Image thickness ~225 nm
<b>Supp.</b> <b>Fig. 4</b>	BS-C-1 cell, wildtype	Extracted, then PFA/GA	Rat × Tub	D × Rat DNA		Overnight	
<b>Supp.</b> <b>Fig. 5</b>	BS-C-1 cell, wildtype	Extracted, then PFA/GA	Rat × Tub	Ms × Rat Alexa 647 (~5.3 d/p) 3° Ab D × Ms Atto 488 (~6 d/p)	0.25% GA 10 min	Overnight	Pre-expansion localization microscopy with 100× 1.45NA TIRF lens; post-expansion imaging by epifluorescence with 60× 1.2NA water lens
<b>Supp.</b> <b>Fig. 9</b>	BS-C-1 cells: <b>a-d)</b> wildtype; expressing <b>e)</b> mito-GFP or <b>f)</b> Sec61β-GFP	<b>a-b)</b> extracted, fixed with PFA/GA <b>c-f)</b> not extracted, fixed with PFA/GA	<b>a)</b> Rat × Tub <b>b)</b> Ms × Vim <b>c)</b> Rb × TOM20 <b>d)</b> Rb × PMP70 <b>e,f)</b> Rb × GFP	<b>a)</b> D × Rat Atto 488 (4-6 d/p) <b>b)</b> D × Ms Atto 488 (4-6 d/p) <b>c)</b> D × Rb Atto 488 (4-6 d/p) <b>d)</b> D × Rb Atto 488 (4-6 d/p) <b>e,f)</b> D × Rb Atto 488 (4-6 d/p)	0.25% GA 10 min	Overnight	Epifluorescence, 60× 1.2NA water lens
<b>Supp.</b> <b>Fig. 10</b>	BS-C-1 cells, wildtype	Extracted, then PFA/GA	Rat × Tub	<b>a-b)</b> D × Rat Atto 488 (~8 d/p) <b>c)</b> D × Rat DNA (2.25 µg/mL) + 1 µM acrydite-DNA-Atto 488	<b>a)</b> 0.25% GA 10 min <b>b)</b> 25 mM MA-NHS 60 min <b>c)</b> no post-stain linking	Overnight	Epifluorescence, 60× 1.2NA water lens
<b>Supp.</b> <b>Fig. 11</b>	BS-C-1 cells, wildtype and expressing mito- GFP	Not extracted, fixed with PFA/GA	Rb × TOM20 for antibody measurements	D × Rb Atto 488 (~8 d/p) D × Rb DNA (2.25 µg/mL) + 1 µM acrydite-DNA-Atto 488	Either 0.25% GA 10 min, 25 mM MA-NHS 60 min, or no post-stain linking (DNA)	Both GA: 30 min Antibody MA and DNA: overnight	Epifluorescence, 20× 0.45 NA air lens. Detected antibody or intrinsic GFP signal as indicated.
<b>Supp.</b> <b>Fig. 12</b>	BS-C-1 cells, wildtype	Extracted, then PFA/GA	Rat × Tub	<b>a)</b> D × Rat Atto 488 (~8 d/p) <b>b)</b> D × Rat Alexa 488 (~8 d/p, commercial)	0.25% GA 10 min	Overnight	Epifluorescence, 60× 1.2NA water lens
<b>Supp.</b> <b>Fig. 13</b>	BS-C-1 cells, wildtype	Extracted, then PFA/GA	Rat × Tub	D × Rat Atto 488 (~8 d/p)	0.25% GA 10 min	<b>a)</b> No digestion, <b>b)</b> 30 min, <b>c)</b> 18 h	Epifluorescence, 60× 1.2NA water lens
<b>Supp.</b> <b>Fig. 14</b>	BS-C-1 cells, wildtype	Extracted, then PFA/GA	Rat × Tub	D × Rat Atto 488 (~8 d/p)	25 mM MA-NHS 60 min	<b>a)</b> No digestion, <b>b)</b> 2h, <b>c)</b> 18 h	Epifluorescence, 60× 1.2NA water lens
<b>Supp.</b> <b>Fig. 15</b>	BS-C-1 cells expressing Sec61β- GFP	PFA/GA, 37 °C	--	--	Initial fixation included 0.1% GA for 10 min	<b>a)</b> 30 min, <b>b,c)</b> 18 h	Epifluorescence, 60× 1.2NA water lens. Detected intrinsic GFP signal.
<b>Supp.</b> <b>Fig. 16</b>	BS-C-1 cells expressing mito-GFP	<b>a)</b> PFA/GA <b>b,c)</b> PFA	--	--	Initial fixation included 0.1% GA for 10 min	30 min	Epifluorescence, 60× 1.2NA water lens. Detected intrinsic GFP signal.
<b>3 a-f</b>	THY1-YFP-H mouse brain, 100 µm slice	Cardiac perfusion with PFA, then 1 h PFA after slicing	Ch × GFP Rb × Homer Ms × Bassoon	<b>a)</b> D × Ch Atto 488 (~6 d/p) <b>b)</b> D × Rb Atto 647N (~2.7 d/p) <b>c)</b> D × Ms Atto 565 (~5.2 d/p)	1 mM MA-NHS 60 min	Digestion: overnight	Confocal, 25× 1.0 NA water SCALE lens. Image thicknesses: <b>a)</b> ~1.2 µm (single z-plane); <b>b)</b> ~3.8 µm; <b>c- d)</b> ~1.2 µm (single z-plane); <b>e, f)</b> 1.4 µm.
<b>3 i-j</b>	THY1-YFP-H mouse brain, 100 µm slice	Cardiac perfusion with PFA, then 1 h PFA after slicing	--	--	1 mM MA-NHS 60 min	60 min	Epifluorescence, 20× 0.45NA air lens
<b>Supp.</b> <b>Fig. 17</b>	THY1-YFP-H mouse	Cardiac perfusion with PFA, then 1 h PFA after slicing	Rb × GFP	D × Rb Atto 488 (~9 d/p)	<b>a)</b> 1 mM MA-NHS 60 min <b>b)</b> 0.1% GA 10 min	Overnight	Epifluorescence, 10× 0.25 NA air lens
<b>Supp.</b> <b>Fig. 18,</b> <b>Supp.</b> <b>Vid. 1</b>	THY1-YFP-H mouse	Cardiac perfusion with PFA, then 1 h PFA after slicing	Ch × GFP Rb × Homer Ms × Bassoon	<b>a)</b> D × Ch Atto 488 (~6 d/p) <b>b)</b> D × Rb Atto 647N (~2.7 d/p) <b>c)</b> D × Ms Atto 565 (~5.2 d/p)	1 mM MA-NHS 60 min	Digestion: overnight	Confocal, 25 × 1.0 NA water lens. Image thicknesses: <b>a)</b> 0.8 µm; <b>c)</b> 1.6 µm; <b>e)</b> 1.8 µm; <b>g)</b> 2 µm; <b>i)</b> 2.2 µm.
<b>Supp.</b> <b>Fig. 19</b>	THY1-YFP-H mouse	Cardiac perfusion with PFA, then 1 h PFA after slicing	Ch × GFP Rb × Homer Ms × Bassoon	<b>a)</b> D × Ch Atto 488 (~6 d/p) <b>b)</b> D × Rb Atto 647N (~2.7 d/p) <b>c)</b> D × Ms Atto 565 (~5.2 d/p)	1 mM MA-NHS 60 min	Digestion: overnight	Confocal, 25 × 1.0 NA water lens. Image thicknesses: 13.2 µm
<b>Supp.</b> <b>Fig. 20</b>	THY1-YFP-H mouse	Cardiac perfusion with PFA, then 1 h PFA after slicing	--	--	<b>a)</b> 1 mM MA-NHS 60 min <b>b)</b> No treatment	Digestion: overnight	Epifluorescence, 20× 0.45 NA air lens. Detected intrinsic YFP signal.
<b>Supp.</b> <b>Fig. 21</b>	BS-C-1 cells, wildtype	Extracted, then PFA/GA	Rat × Tub for tubulin stains only	<b>a)</b> Hoechst (2 drops/mL) <b>b)</b> D × Rat Alexa 405 (~3 d/p) <b>c)</b> D × Rat Atto 488 (~10 d/p) <b>d)</b> SYBR Gold (10×) <b>e)</b> D × Rat Alexa 546 (~10 d/p) <b>f)</b> D × Rat Atto 647N (~5.5 d/p) <b>g)</b> D × Rat Biotin	<b>a-e)</b> 0.25% GA 10 min	<b>a-f)</b> Overnight digestion <b>g)</b> 1 h digestion. Post-expansion with streptavidin Alexa 647 (3 dyes/SA, 2 µg/mL)	Confocal, 63× 1.2 NA water lens. Image thicknesses: tubulin, 225 nm; nuclei, 7 µm.

**Supplementary Protocol 1.** Detailed protocol for magnification calculation and distortion analysis.

In this manuscript we used the open-source software *Elastix* for analysis of correlated pre- and post-expansion images in order to calculate the physical magnification (referred to as the expansion factor in the main text) and to perform analysis of expansion-related distortions.<sup>2</sup> The output from *Elastix* was further processed using custom-written Mathematica scripts. In this supplementary protocol we provide detailed instructions on how to perform these analyses for a computer based on a Microsoft Windows operating system. This protocol also makes use of the widely used open-source ImageJ-based software package *Fiji* [insert ref here].

This supplementary protocol is accompanied by the file “SupplementaryAnalysis.zip”. The .zip file contains three subfolders: “original\_data” contains original confocal data files for corresponding pre-expansion and post-expansion images; “similarity\_example” contains input files for rigid registration analysis using *Elastix*; “spline\_example” contains input files for distortion analysis with *Elastix* that are derived from the output of the similarity analysis. The spline\_example folder also contains a Mathematica script file (.nb) for processing of the *Elastix* B-spline output file for distortion analysis.

### **Elastix Installation**

The open-source software *Elastix* was used for rigid (similarity) and nonrigid (B-spline) registration of correlated pre- and post-expansion images. *Elastix* may be downloaded from the program’s website at <http://elastix.isi.uu.nl>. Once installed, add the installed *Elastix* directory to the system’s PATH variable. *Elastix* is controlled through the Command Prompt, and the following font and gray background will be used to denote command line inputs: `command line inputs`. To check whether the installation was successful, open a Command Prompt and enter `elastix -help` to see the version and command options (an error is returned if the installation was unsuccessful or if *Elastix* directory has not been added to the PATH variable). For more detailed information on installation, information about image registration, and all further procedures, consult the *Elastix* manual found on the homepage. The *Elastix* parameter database also has helpful example parameter files for analysis ([http://elastix.bigr.nl/wiki/index.php/Parameter\\_file\\_database](http://elastix.bigr.nl/wiki/index.php/Parameter_file_database)).

### **Image Data Formatting Preparation**

*Elastix* is based on the Image Registration and Segmentation Toolkit (ITK), and therefore all input/output image files must be compatible with ITK, such as .mhd or .mha files that store image data in uncompressed binary format. It is convenient to use other imaging applications such as *Fiji* (<http://fiji.sc/Fiji>)<sup>3</sup> to create or view these binary image files. To create binary image files for our sample pre-expansion data located in the original\_data folder, perform the following steps: 1) Load the example pre-expansion data file “Pre\_ExM.tif” (a 128 × 128 pixel 16

bit TIFF) into *Fiji*; 2) Use bicubic interpolation to resample the image with 4× smaller pixels (Image → Scale... → X Scale = 4, Y Scale = 4), resulting in a 512 × 512 image, so that the pre-expansion data will have approximately the same scale as the post-expansion data; 3) Save the image as a binary file by selecting (File → Save As... → Raw Data...), and name it “fixed.raw”; 4) Manually create a “.mhd” metadata file (Metimage medical data) that contains the information shown below. The binary image file and metadata files generated according to this procedure are included in the similarity\_example folder as “fixed.raw” and “fixed.mdh”, respectively.

```
ObjectType = Image
NDims = 2
BinaryData = True
BinaryDataByteOrderMSB = True
ElementSpacing = 1 1
DimSize = 512 512
ElementType = MET_USHORT
ElementDataFile = fixed.raw
```

Follow a similar procedure to create a binary image file and metadata file for the example post-expansion image “Post\_ExM.tif” (a 512 × 512 pixel 16 bit TIFF), but omitting the bicubic interpolation step. These binary image and metadata files are included in the similarity\_example folder as “moving.raw” and “moving.mdh”, respectively.

*Troubleshooting note regarding file formats:* Depending on the software and/or computer preferences for byte order (i.e., “endianness”), the .mdh metadata parameter BinaryDataByteOrderMSB may need to be changed to either True or False in order to be loaded properly by *Elastix*. In *ImageJ* and *Fiji*, “Raw Data...” export should default to big-endian byte order and the BinaryDataByteOrderMSB option should be set to True in the .mhd file. Validate the byte ordering is correct by loading the “.mhd” file into *Fiji*; when correctly formatted, the original images should appear normally as shown in Appendix Figure 1a and b (i.e., not scrambled). The initial overlay should be roughly the same region and scaling as in Appendix Figure 1c).

### **General *Elastix* Usage: Similarity Transform**

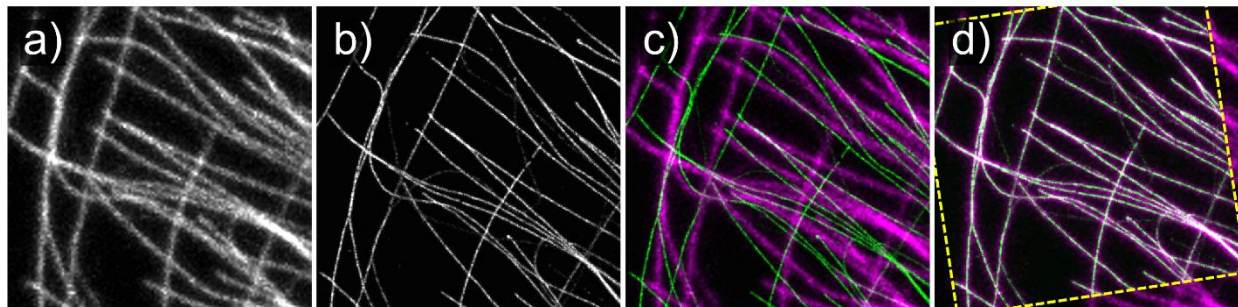
*Elastix* compares two input images, denoted the fixed image and the moving image, and will attempt to rigidly or nonrigidly transform the moving image so that it matches the fixed image file. Example files are provided in the similarity\_example and spline\_example folders. The example files in each folder include a fixed image, a moving image, the corresponding .mhd metadata files, and an *Elastix* parameter files.



In this example, we will use the parameter file “Parameters\_Similarity.txt” provided in the example files. To run *Elastix*, open a Command Prompt inside the “similarity\_example” folder by pressing together *Shift + Right Click*, selecting “Open command window here”, and entering:

```
elastix -f fixed.mhd -m moving.mhd -p Parameters_Similarity.txt -out .
```

The *-f* and *-m* indicate the fixed and moving image “.mhd” input files, the *-p* indicates the parameters input file, and *-out* indicates where the output files will be written. The period (.) after *-out* is shorthand for the current directory of the command prompt, however any valid path will work. In general, use file names that do not contain spaces (underscores are acceptable), or alternatively enclose names or full file paths with quotation marks. After *Elastix* finishes running, an output binary image file “result.0” and its corresponding “result.0.mhd” file should be generated. Check the output image by dragging the “result.0.mhd” file into *Fiji*. Overlay the fixed and result.0 images to display the registration result, as displayed in Appendix Figure 1d. Note that signedness of the output (MET\_SHORT) is different from the input (MET\_USHORT) and is specified in corresponding .mhd files; however the output will be displayed correctly when opened with *Fiji*.



**Appendix Figure 1.** The “fixed” pre-expansion (a) and “moving” post-expansion (b) images to be registered by *Elastix*. The initial unregistered overlay (c) and overlay after *Elastix* similarity registration (d). The pre-expansion images are displayed in magenta and the post-expansion images in green. The dotted yellow lines in (d) outline the edges of the post-expansion image and have been added to emphasize the transformation.

*Troubleshooting notes regarding Elastix command line usage.* If *Elastix* does not run, observe the error output in the command window, or look for the “elastix.txt” output file, which should also contain the error. Common errors include incorrect input of file names into the command line, file names containing spaces, or an incorrect “ElementDataFile” name referencing the binary data in the .mhd file. Additionally, be wary of extra file extensions that

may become appended (particularly in Windows), but appear hidden on the .raw and .mhd files, which will cause *Elastix* to respond with an error.

### **Expansion Factor Determination with *Elastix***

The similarity transformation (used in the previous example) attempts to match the moving image to the fixed image using only rotation, translation and isotropic scaling; and can therefore be used to calculate the isotropic expansion factor. In the previous example, the pre-expansion image was interpolated by a factor of 4; this factor was the estimated expansion factor determined macroscopically with a ruler (by measuring the size of the gel in millimeters before and after expansion). All ExM samples in this work had expansion factors ranging from 4.0-4.3, so a flat factor of 4 is a good initial guess for the similarity transform. Even this type of rough macroscopic measurement can yield results accurate to within 5-10% of the true expansion factor. Note, if the images were acquired with different pixel sizes (such as on a confocal microscope with adjustable magnification), it is convenient to first interpolate one of the images to match the smaller pixel size of the two; this is unnecessary if images were acquired with the same pixel size, such as on a CCD/CMOS array using the same objective lens. After successfully performing the similarity transform and ensuring proper registration of the two images, as in Appendix Figure 1d, look for the output text file named “TransformParameters.0.txt” which contains the following parameters of the similarity transform at the top of the document:

```
(Transform "SimilarityTransform")  
(NumberOfParameters 4)  
(TransformParameters 1.029177 0.163145 13.092766 17.873457)  
(InitialTransformParametersFileName "NoInitialTransform")  
(HowToCombineTransforms "Compose")
```

The key numbers are the TransformParameters, which represent the image scaling factor, rotation, translation in X, and translation in Y, respectively. The transformation is applied to the moving image (post-expansion image) and since the pre-expansion image was previously interpolated by the estimated factor of 4, this factor is multiplied by the scaling factor to get the true expansion factor:  $4 \times 1.03 = 4.12$ .

**Troubleshooting Similarity Transform.** If the similarity transformation does not return acceptable registration, it is useful to first try and select corresponding areas of the input pre-expansion and post-expansion images to be as close as possible by eye before running *Elastix*. This includes scaling by the estimated expansion factor (as described previously), as well matching the image orientations by rotating one of the images (In *Fiji*, Image → Transform → Rotate...). Additionally it is possible to tune the input parameter file “Parameters\_Similarity.txt”. Some useful parameters to consider are the (NumberOfResolutions 8) or (MaximumNumberOfIterations 1000). *Elastix* will begin initial registration at a reduced

image resolutions and increasing to full resolution, (by default each resolution to run is decreased by factor of 2), unless otherwise specified in the parameters file, and the `MaximumNumberOfIterations` will allow for convergence during each resolution. These parameters are set initially at higher values for more robust registration, however often times if the initial input images are similar, the number of resolutions and max iterations can be decreased to save computation time. Note that the similarity transform is a rigid transform, and only performs uniform scaling in X and Y, rotation and translation. If the scaling in X and Y are not uniform, which is typically not the case for ExM (unless for example, the gel is being stretched or imaging during pre- and post-expansion imaging was not performed on the same axis), it may be necessary to use an affine registration by changing the (Transform "Similarity") to (Transform "AffineTransform") in the parameters file.

### **Nonrigid B-spline Registration with *Elastix***

The similarity transform is a rigid registration and attempts to make a global best match, but correct for local deviations from the fixed image, making it necessary to apply a nonrigid bspline registration. Essentially, the output of the similarity transform is plugged back into *Elastix* as the moving image, and a second registration using B-spline parameters is used to correct for nonrigid deformations that may be present between the pre-expansion and post-expansion, similarity transformed output image. The data for this example is in the "spline\_example" folder, and should contain a fixed and moving binary data files and corresponding .mhd files, as well as a "Parameters\_BSpline.txt" file. Although the files are already included, the "moving" and "moving.mhd" are simply copies of "result.0" and "result.0.mhd" from the "similarity\_example" folder, and renamed accordingly (it is important to change the `ElementDataFile` name in the .mhd as well). The Command Prompt input to run this parameter set in the spline\_example folder is:

```
elastix -f fixed.mhd -m moving.mhd -p Parameters_BSpline.txt -out .
```

The resulting image "result.0" should show only minor deformation when overlayed with the input "moving" image. Further processing to create the deformation vector field plot and measurement RMS error plot using the output B-spline transformation parameters is possible using another program included in the *Elastix* installation called *Transformix*.

### **Vector Fields and RMS error Error using *Transformix* Output**

*Transformix* is a complementary program to *Elastix* that is used to apply a deformation to an image, or a list of XY coordinates. The deformation information is contained within the "TransformParameters.0.txt" files. Here, *Transformix* is used to apply a deformation to a set of input points (an example of using *Transformix* on an image file is provided later). Due to the more advanced formatting, parsing and plotting requirements of the input and output data with *Transformix*, an example *Mathematica* notebook "Vector and RMS plot.nb" is included to generate the deformation vector field plots, as well as measure the RMS error (as in

**Supplemental Fig. 3**). The script is commented to contain instructions.

Briefly described here, to create the vector plot, the deformation field is applied to an input array of points sampled at a set interval, in this case every 10 pixels. *Transformix* is used to deform these input points, and the deformation vector at each point is then used to make a plot of the deformation field. The Command Prompt input to run *Transformix* on set of input points is:

```
transformix -def inputPoints.txt -out . -tp TransformParameters.0.txt
```

The input points should be formatted as follows (see “inputPoints.txt” file in the spline\_example folder):

```
Index
Total # of points
X1 Y1
X2 Y2
... ..
```

To generate the measurement RMS error plots, a similar procedure to the vector plot is used, however the input points are the coordinates of a binary skeleton of the fixed image. In the script, the distance between a pair of points is calculated ( $m$ ), as is the distance between the deformed coordinates ( $m'$ , see **Supplemental Fig. 3**). The absolute value of the difference is the error. This is performed for all combinations of input coordinates in the image skeleton, and RMS error is calculated and plotted.

### Gaussian Blurring of Post-ExM Images

For the sake of simplicity in the previous examples, the following steps on Gaussian blurring of the initial moving image were excluded from this protocol, but were carried out in analysis in the Supplemental Figures. When comparing the pre-expansion and post-expansion example images (in these examples, microtubules), there is a disparity in the microtubule width between the two, due to the increase in resolution in post-expansion space. To ensure that this width disparity does not affect the similarity or Bspline registration process, we first apply a Gaussian blur to the post-expansion image in *Fiji* (Process → Filters → Gaussian Blur... → Radius = 4) to make the microtubule widths roughly equivalent, then proceed with this blurred image as the moving image in similarity registration and subsequently, the blurred similarity output in the Bspline registration. Once the transformation parameters have been determined, the deformations can be applied to the original, unblurred image using *Transformix*. By using the following command:

```
transformix -in unblurred.mhd -out . -tp TransformParameters.0.txt
```

where the unblurred.mhd file corresponds to the original unblurred moving image, and “TransformParameters.0.txt” correspond to the similarity transform parameters output in the

“similarity\_example” folder. The *Transformix* output will be called “result” and “result.mhd”; these images are then plugged back into *Transformix* using the B-spline output parameters in the “spline\_example” folder likewise.

### 3D Registration in *Elastix*

Rigid and nonrigid registration is easily extended into three dimensions using the earlier procedures with minor changes. Beginning from an image stack (assume a  $512 \times 512 \times 128$  pixel image) in *Fiji*, save the data as “Raw Data...” as done previously. The corresponding metadata .mhd must be modified to contain:

```
ObjectType = Image
NDims = 3
BinaryData = True
BinaryDataByteOrderMSB = True
ElementSpacing = 1 1 1
DimSize = 512 512 128
ElementType = MET_SHORT
ElementDataFile = moving.raw
```

The important fields to update are the NDims = 3, to denote three dimensional data, and DimSize with the appropriate image dimensions (in this case, the 128 refers to the number of z-planes). Again, it is helpful to check that the metadata file is correct by dragging it into *Fiji* and checking if the image opens correctly. Finally, change the *Elastix* parameter files (“Parameters\_Similarity.txt” or “Parameters\_Spline.txt”) FixedImageDimension and MovingImageDimension fields to read:

```
(FixedImageDimension 3)
(MovingImageDimension 3)
```

Once these changes to the metadata and parameters files are made, *Elastix* can be called from the command line in the familiar manner.

### Concluding Remarks

In general, due to the large amount of book-keeping involved for image, metadata and *Elastix* outputs files, we recommend running *Elastix* using a user preferred scripting language to automate the process, such as *Mathematica*, *MATLAB*, *Python*, etc. Many of these tools are already in existence, refer to Additional Tools on the Elastix Wiki (<http://elastix.isi.uu.nl/wiki.php>) or SimpleElastix (<http://simpleelastix.github.io>). This protocol and basic command line usage is meant to serve as a primer for using *Elastix* with correlative expansion microscopy.

## REFERENCES

1. Chen, F., Tillberg, P. W. & Boyden, E. S. Expansion microscopy. *Science* **347**, 543–548 (2015).
2. Klein, S., Staring, M., Murphy, K., Viergever, M. A. & Pluim, J. elastix: A Toolbox for Intensity-Based Medical Image Registration. *IEEE Trans. Med. Imaging* **29**, 196–205 (2010).
3. Schindelin, J. *et al.* Fiji: an open-source platform for biological-image analysis. *Nat. Methods* **9**, 676–682 (2012).